Significantly shorter Fe-S bond in cytochrome P450-I is consistent with greater reactivity relative to chloroperoxidase

Courtney M. Krest[a], **Alexey Silakov**, **Jonathan Rittle**, **Timothy H. Yosca**, **Elizabeth L. Onderko**, **Julio C. Calixto**, and **Michael T. Green**[*]

Department of Chemistry, Penn State University, University Park, PA 16802

Abstract

Cytochrome P450 (P450) and chloroperoxidase (CPO) are thiolate ligated heme proteins that catalyze the activation of carbon hydrogen bonds. The principal intermediate in these reactions is a ferryl radical species called compound I. P450 compound I (P450-I) is significantly more reactive than CPO-I, which only cleaves activated C-H bonds. To provide insight into the differing reactivities of these intermediates, we examined CPO-I and P450-I with variable temperature Mössbauer and X-ray absorption spectroscopies. These measurements indicate that the Fe-S bond is significantly shorter in P450-I than in CPO-I. This difference in Fe-S bond lengths can be understood in terms of variations in hydrogen bonding patterns within the "cys-pocket" (a portion of the proximal helix that encircles the thiolate ligand). Weaker hydrogen bonding in P450-I results in a shorter Fe-S bond, which enables greater electron donation from the axial-thiolate ligand. This observation may in part explain P450's greater propensity for C-H bond activation.

There has been considerable interest in the role that cytochrome P450's unusual thiolate ligand plays in catalysis.[1] Only thiolate ligated heme proteins are known to activate C-H bonds, suggesting a critical role for the ligand in this process. Strong electron donation from the axial thiolate has been proposed to facilitate both oxygen and C-H bond activation.[2-6]

The principal intermediate in P450 catalysis is a high-valent ferryl radical species called compound I (P450-I). Until recently, the reactive nature of this intermediate precluded its electronic and structural characterizations.[5,7-9] As a result, researchers often turned to model systems for insight into P450 chemistry. Important in this regard have been studies with synthetic metal-oxo porphyrins.[10-16]

Investigations with these systems have shown that reactivity with respect to oxygen transfer increases with electron donation from the axial ligand.[10-14] These studies have typically

[*]Correspondence and requests for materials should be addressed to M.T.G..

[a]Current address: Stanford Synchrotron Radiation Lightsource, SLAC National Accelerator Laboratory, Menlo Park, California, 94025

involved synthetic iron porphyrins coordinated by a series of hard ligands (e.g. F⁻, Cl⁻, AcO⁻, CF$_3$SO$_3$⁻). Synthetic systems with thiolate ligation are rare, but Nagano and Higuchi reported an iron porphyrin (the "Swan-Resting", S.R.) complex, which can be prepared with either thiolate or imidazole axial ligation.[15,16] In competitive oxidations of cyclooctane and cyclooctene, the thiolate ligated S.R. complex was found to be an order of magnitude more likely to perform C-H bond activation than the imidazole ligated system, supporting a unique role for P450's axial thiolate ligand.[16]

The thiolate ligated heme enzyme chloroperoxidase (CPO) has proven to be another important model system for the study of P450 chemistry.[2] CPO's main function is thought to lie in the incorporation of chloride into the antibiotic caldariomycin, but the enzyme is also known to hydroxylate a range of *activated* hydrocarbons (BDFE 91 kcal/mol).[17] Chloroperoxidase compound I (CPO-I) is relatively stable (compared to P450-I) permitting early spectroscopic characterizations of CPO-I that have provided valuable insight into the electronic and geometric structures of a thiolate ligated compound I.[18,19]

There is an important difference, however, between CPO and P450: CPO does not oxidize unactivated hydrocarbons, such as cyclohexane (BDFE ~ 101 kcal/mol).[17] It is possible that this difference in reactivity may be linked, at least in part, to substrate access. P450s have large flexible substrate binding pockets, providing ready access to targeted C-H bonds, while entry to the CPO-I active site appears to be more limited.[20,21] Evidence suggests, however, that more than substrate access is at play.[22,23] CPO-I epoxidizes terminally unsaturated fatty acids, indicating that the molecules' aliphatic termini can reach the ferryl moiety. Yet, as we will show, the reaction with fully saturated fatty acids is not observed.

The disparity in C-H bond hydroxylation competence suggests an inherent difference in the reactivity of compound I in P450 and CPO. This raises an interesting question: Is P450's greater propensity for C-H bond activation consistent with the insights gained from synthetic model compounds? Is the thiolate ligand more donating in P450? P450 and CPO have distinct protein folds with different hydrogen-bonding patterns to the thiolate.[20] The ability of these non-covalent interactions to tune the electronic properties of the axial ligand has been a topic of interest and debate.[24-33]

X-ray crystallography has revealed that, in both systems, the proximal thiolate sits in what has been termed the "cys-pocket". The residues directly following the cysteine coil around the thiolate, presenting amide N-H's for hydrogen bonding to the thiolate ligand. The cys-pocket of CPO and P450 are shown in Figure 1.[20,21,34,35] Comparison reveals that CPO has one less amide N-H available for hydrogen bonding to the thiolate. As result, it has been thought that H-bonding to the axial thiolate is stronger in P450 than in CPO.[28] However, magnetic circular dichroism (MCD) experiments suggest that at least two of P450's putative hydrogen bonds may have little effect on the electronic structure.[32,33]

Recently, we reported that compound I could be prepared in three different P450s, in CYP119A1 and CYP119A2 from the thermophillic organisms *Sulfolobus acidocaldarius* and *Sulfolobus tokodaii*, and a Y352F CYP158A2 variant (CYP158A2*) from *Streptomyces coelicolor*, in which tyrosine 352 was replaced with a phenylalanine.[5-7] This has opened the

door for detailed spectroscopic characterizations of P450-I, facilitating crucial comparisons with CPO-I. Spectroscopic measurements indicate that |J/D|, the ratio of the exchange coupling to the zero-field splitting, is ~30% larger in P450-I than CPO-I (1.3 vs. 1.0).[5] This increase in |J/D| suggests a significant difference in the electronic and/or geometric structures of these intermediates. In an effort to provide insight, we have performed variable temperature Mössbauer and Fe K-edge X-ray absorption measurements on CPO-I and P450-I. These measurements suggest weaker hydrogen bonding to and greater electron donation from the thiolate in P450.

Results

Stopped-Flow Kinetics Measurements

Direct comparisons of rates of substrate oxidation by P450-I and CPO-I have not been made. Here we compare the reactivity of CPO-I and CYP119A1-I with hexanoic and 5-hexenoic acid. Stopped-flow measurements indicate that CPO-I readily reacts with 5-hexenoic acid with a rate constant of 7×10^3 M^{-1}s^{-1} at 4°C.[36] However, no reaction is observed with hexanoic acid. In contrast, CYP119A1-I oxidizes both hexanoic acid and 5-hexenoic acid at rates of 4×10^4 and 3×10^5 M^{-1}s^{-1} at 4°C, respectively (Figure 2).

Variable Temperature Mössbauer (VTM) Measurements

Compound I is best described as having an S=1 iron(IV)oxo unit exchange coupled to an S=1/2 ligand-based radical.[5] The location of this radical in P450s (on the thiolate, the porphyrin, or some mixture of both) is an important and unresolved question in the field, with implications for reactivity and the reliability of quantum chemical calculations. The exchange coupling (J) between the iron(IV)oxo unit and the ligand-based radical produces doublet and quartet states, which are mixed by the zero-field splitting (D) of the ferryl moiety, resulting in three Kramers doublets.[5,18]

Thiolate ligation is known to affect the exchange coupling of compound I. EPR measurements on CPO-I have revealed strong antiferromagnetic coupling between the S=1 ferryl moiety and the S=1/2 radical (|J| = 35 cm^{-1} for CPO-I).[18] Synthetic model complexes have strong ferromagnetic interactions with |J| values ranging between 25 and 60 cm^{-1}, while the coupling in histidine ligated peroxidases is weakly ferromagnetic, |J| = 0-10 cm^{-1}.[37-39] It has been suggested that antiferromagnetic coupling in the thiolate ligated systems can be understood in terms of delocalization of the porphyrin radical onto the axial ligand.[39,40]

EPR measurements have shown that |J/D| is ~30% larger in P450-I than in CPO-I. A larger value of |J| could be the hallmark of increased sulfur spin density and/or a shortened Fe-S bond, both of which would suggest increased electron donation from the axial thiolate ligand. The magnitudes of J and D cannot be determined directly from CW EPR experiments, but they can be obtained from relaxation studies. Between 10 and 60 K, electronic relaxation in compound I proceeds predominantly through an Orbach mechanism.[18] T$_1$ (the electronic relaxation time) is determined by   , the energy splitting between the middle and ground Kramers doublets (Eq. 1). Because   is solely a function of

J and D (Eq. 2), and the value of J/D is known from EPR, T_1 measurements can uniquely determine J and D.

$$W\left(T\right)=1/T_1\left(T\right)=A\Delta^3\frac{1}{exp\left(\Delta/T\right)-1}\quad\text{(Eq. 1)}$$

where A is a system-dependent constant (mm s^{-1} K^{-3}), T is the temperature (K), and   is given by,

$$\Delta=\frac{1}{2}*\sqrt{9J^2-4DJ+4D^2}\quad\text{(Eq. 2)}$$

This result, which assumes axial symmetry ($E/D = 0$), was obtained from the following spin Hamiltonian:

$$\hat{\mathscr{H}}_S=D\left(\hat{S}_{1z}^2-2/3\right)+J\hat{S}_1\bullet\hat{S}_2\quad\text{(Eq. 3)}$$

where $\hat{S}_1$ and $\hat{S}_2$ are the spin operators for the ferryl moiety and ligand-based radical, respectively. $J > 0$ indicates antiferromagnetic coupling.

Typically, measurements of the electronic spin relaxation rates are performed using EPR methods. However, in the current case, we have found ^{57}Fe Mössbauer spectroscopy to be more suitable, as it gives a wider accessible temperature range and thus improved quality of data analysis. Figure 3 shows that the Möossbauer spectrum of compound I collapses to a quadrupole doublet as the temperature increases above 4.2 K. This collapse is due to the "averaging-out" of the magnetic interactions between the electronic spin and the ^{57}Fe nucleus as the electronic relaxation rate ($1/T_1$) approaches and exceeds the intrinsic width of the Mössbauer transition ($\sim 10^7$ s^{-1}).[41] It is clear from the spectra shown in Fig. 3 that CYP119A1-I relaxes more slowly than CPO-I.

Mössbauer spectra are typically fit in the slow (not averaged-out) or fast (completely averaged-out) relaxation regimes. However, it has been shown that intermediate relaxing spectra can be analyzed to obtain electronic relaxation rates.[41,42] To extract the relaxation rates from the Mössbauer spectra, fits of the 4.2 K data were first performed to obtain Mössbauer parameters in the slow relaxation limit. For fits of intermediate relaxing data (Fig. 3 and Supplementary Tables S1 and S2), the Mössbauer parameters were constrained to the values obtained at 4.2 K: Only the electronic relaxation rate ($W=1/T_1$) was allowed to vary. As can be seen from Fig. 3C, for most of the temperature range, the data show a logarithmic dependence on the inverse temperature ($1/T$), which is well modeled by an Orbach process. Best fits to Eq. 2 provide the following   values:

$$\Delta_{CYP_{119A_1-I}}=110\pm5\quad\text{K}$$
$$\Delta_{CPO-I}=84\pm3\quad\text{K.}$$

Inserting   and the ratio |J/D| into Eq. 2 yields the following values for J and D:

$$D_{CYP_{119A_1}-I} = 40 \quad cm^{-1} \quad (58 \quad K), \quad J_{CYP_{119A_1}-I} = 52 \quad cm^{-1} \quad (76 \quad K);$$
$$D_{CPO-I} = 39 \quad cm^{-1} \quad (56 \quad K), \quad J_{CPO-I} = 40 \quad cm^{-1} \quad (57 \quad K);$$

The values obtained for CPO-I are in reasonable agreement with those reported previously (D = 52 K, J = 53 K).[18] Our measurements indicate that the zero-field splitting is similar in CPO-I and P450-I. The variation in |J/D| results almost exclusively from a difference in the exchange coupling. The larger J in P450-I suggests greater spin density on the axial thiolate and/or a shorter Fe-S bond relative to CPO-I.

X-ray Absorption Measurements

Fe K-edge XANES—XANES data of CPO-I and ferric CPO look similar to those of CYP119A1-I and ferric CYP119A1, respectively (Supplementary Figure S1). The CYP119A1 ferric edge lies ~1.8 eV lower in energy than that of CYP119A1-I, while in CPO this difference was slightly smaller, ~1.6 eV. In both systems, the pre-edge feature resulting from the compound I species is larger and at higher energy than that of the ferric species. The pre-edge feature of CPO-I is noticeably larger than that of the P450-I sample (Supplementary Figure S1). This is due in large part to the presence of ~30% ferric enzyme in the P450-I sample. Fits of the pre-edge features indicate that the pre-edge intensity of CPO-I is 14 ± 8% larger than that of CYP119A1-I (Supplementary Figure S2).[43,44]

Given the magnitude of the uncertainty in the relative intensity, we calculated pre-edge spectra (See Methods section) to determine if the observed metal-ligand bond lengths (discussed below) are consistent with the observed variation in pre-edge intensity. Using methods outlined by DeBeer and Neese,[43] we find that the pre-edge feature in CPO-I is predicted to be ~17% larger than in CYP119A1-I (27 units compared to 23 units, respectively).

Fe K-edge EXAFS—Extended X-ray Absorption Fine Structure (EXAFS) measurements have been performed for both CYP119A1-I and CPO-I to resolve and compare Fe-S and Fe-O bond distances in each species. Multiple measurements were performed (three for CYP119A1-I and four for CPO-I) on independently prepared samples, during different experimental runs.

Figure 4 shows the EXAFS and Fourier transforms for CYP119A1-I and CPO-I. Our analysis of the EXAFS data reveals that the Fe-S bond distance in CYP119A1-I is ~0.10 Å shorter than the Fe-S bond distance in CPO-I (2.388 Å compared to 2.481 Å). In addition, the Fe-O distance in CYP119A1-I is longer (1.670 Å) than in CPO (1.661 Å). Best-fit parameters and 90% confidence intervals for the metal-ligand distances can be found in Table 1.

EXAFS experiments were also performed on compound I intermediates prepared in CYP119A2 and CYP158A2* (Table 1). Averaging all five P450-I measurements yields an Fe-S distance of 2.391 Å and an Fe-O distance of 1.670, essentially identical to the results obtained for CYP119A1. EXAFS measurements of the ferric enzymes produced Fe-S

distances of 2.21 Å for P450 and 2.24 Å for CPO[3] (Supplementary Table S3 and Supplementary Figure S3).

Discussion

Experiments with synthetic metal-oxo complexes have shown that donating axial ligands enhance reactivity with respect to oxygen transfer and C-H bond activation.[10-16] Density functional calculations have linked this increased reactivity to a strengthening of the O-H bond formed during C-H bond cleavage.[13,14] In P450, an increase in the O-H bond strength, D(FeO-H), can be understood in terms of a relative stabilization of the metal-hydroxide (or compound II) species with respect to compound I. This increases the driving force, lowering the activation barrier for H-atom abstraction.

Calculations have shown that D(Fe=O) of compound I and D(FeO-H) of compound II are inversely correlated, with the driving force for H-atom abstraction increasing as the Fe=O bond weakens.[13] The shorter Fe-S bond in P450-I allows for greater electron donation into the ferryl π* orbitals, weakening the Fe=O bond. As a result, the Fe=O bond is longer in P450-I than in CPO-I. Although the difference in Fe=O bond lengths is small, ~0.01 Å on average, it is significant for such a short bond. Importantly, our measurements of the Fe=O bond have a standard deviation of ~0.005 Å.

Recently, we reported a similar bonding pattern in compound II. The Fe-S bond is 0.12 Å shorter in P450-II than in CPO-II, while the Fe-OH bond is 0.02 Å longer.[3,6] The compound II bond distances also appear to be consistent with the known reactivities of these systems. Calculations on ferryl porphyrins have indicated that the activation barrier for H-atom abstraction is inversely correlated to the Fe-O bond length in the transition state, which itself is related to the Fe-OH bond length in compound II.[12] Systems with the most donating ligands were predicted to have the longest Fe-OH bonds and be the most reactive with respect to C-H bond activation.[12]

Given that the local coordination environments in CPO and P450 are identical, why is the Fe-S bond ~0.1 Å shorter in P450? This difference in metal-ligand bonding likely derives from variations in non-covalent interactions in the secondary coordination sphere. It has been thought that H-bonding to the axial thiolate is stronger in P450 than in CPO.[28] However, examination of the crystal structures of the ferric enzymes suggests that this is not the case (Figure 1).[34,35]

Only one of the putative H-bonding interactions in the CYP119A1 structure has an S---H distance (2.55 Å) less than the sum of the respective Van der Waals radii ($r_S^{VDW} + r_H^{VDW} =$ 1.8 Å + 1.2 Å = 3.0 Å), and this H-bonding interaction has an N-H---S angle of ~130°, which is far from the optimal angle of 180°. The two additional S---H interactions in P450 (2 and 4 in Figure 1) have poor angles combined with S---H distances over 3.0 Å, which suggests that their effect on the electronic properties of the thiolate is minimal. This is consistent with the results of magnetic circular dichroism (MCD) experiments on CYP101 variants, in which interactions 2 and 4 were individually removed through proline substitution.[32] In contrast to P450, the ferric CPO structure shows a strong H-bonding

interaction with an S---H distance of 2.33 Å and an N-H---S angle of 172°. Notably, the weakest H-bonding interaction in CPO is comparable to the best interaction in P450.

Importantly, the hydrogen-bonding observed in the CYP119A1 structure is typical of P450s (Figure 1 caption). P450s have a unique protein fold with a conserved orientation of the proximal helix that forms the cys-pocket. The different hydrogen-bonding patterns observed in CPO and P450 are dictated by the orientation of this helix. In P450s, the proximal helix runs parallel to the heme plane, while in CPO the helix is almost perpendicular to the porphyrin (Figure 1).[20] In the latter orientation, the axial thiolate caps the alpha helix, allowing for greater interaction with the amide protons as well as inductive effects, which could further strengthen the non-covalent interactions. While one does not expect H-bonding metrics in other (i.e. non-ferric) forms of these enzymes to be identical to those reported in Figure 1, one does expect variations in hydrogen-bonding due to the orientation of the proximal helix to persist. Indeed, this is consistent with resonance Raman experiments on the ferrous-CO adducts of CPO and P450 as well as EPR measurements on the ferric enzymes, both of which suggest greater hydrogen bonding in CPO.[45-47]

The Fe-S bond length of thiolate ligated iron porphyrins is known to increase with increasing H-bonding.[25,48] This is consistent with our EXAFS measurements. The weaker H-bonding in P450 (allowing for greater electron donation from the axial thiolate) may in part explain the enzyme's greater propensity for C-H bond activation. Recall that $|J|$ is 30% larger in P450-I than in CPO-I. Our data suggest that $|J|$ is correlated with the Fe-S distance, and, as such, may be used to gauge electron donation from the axial ligand. An increase in $|J|$ is consistent with a shorter Fe-S distance and/or increased axial ligand spin density. Efforts to quantify the latter are underway.

Methods

Materials

meta-chloroperbenzoic acid (*m*-CPBA, <77%, Aldrich) was purified to 99% following established techniques.[6] Peracetic acid was obtained from Sigma Aldrich and acetonitrile from EMD. All buffers were prepared by standard techniques and the pH was measured at 4°C. Given that our EXAFS and Mössbauer experiments were performed at low temperature a quick comment about the temperature dependence of buffer pH is warranted. It is known that buffer pH can vary significantly with temperature. The pH of 100 mM Tris buffer, for example, changes by +2.3 units on going from 293 K to 77 K, while the pH of 100 mM phosphate buffer changes by approximately two units in the opposite direction.[49] It is less well known, however, that concentrated (~ mM) protein solutions can 'buffer the buffer' against these temperature-dependent changes. Addition of 600 μM bovine serum albumin to the same Tris and phosphate buffers effectively abolishes the temperature dependence of the pH: the pH changes by +0.1 units over the same temperature range.[49] Our recent measurements of the P450-II pK_a are in agreement with this result.[6] Using Mössbauer (4.2 K) and stopped-flow UV/Visible absorption (277 K) spectroscopies, we obtained the same pK_a (±0.1 units) at these vastly different temperatures, indicating that the pH of our samples was not significantly changed upon freezing.

Purification of CYP119A1 and CYP119A2

CYP119A1 and CYP119A2 were overexpressed in BL21-CodonPlus-RIL cells. Protein was purified as reported previously.[5] A Source 30Q column was substituted for the PBE94 chromatofocusing column employed by Ortiz de Montellano and coworkers. Only protein fractions with a purity ratio R_Z (Abs_{416nm}/Abs_{280nm}) of   1.65 were collected, pooled, and used for experiments.[5]

CYP119A1-I and CYP119A2-I Preparation

Both CYP119A1-I and CYP119A2-I samples were prepared as previously described with slight modifications by reacting ~6 mM ferric protein in 100 mM potassium phosphate buffer at pH 7 with ~24 mM *m*-CPBA in 30% acetonitrile in water, in a 2:1 mixture.[5] The aqueous reaction mixture was sprayed into liquid ethane (90 K) ~2 ms after mixing. Liquid ethane was subsequently removed under vacuum in an isopentane bath (~128 K), after which samples were packed into Mössbauer or EXAFS cups under liquid nitrogen. Both CYP119A1-I and CYP119A2-I samples contained ~30% ferric enzyme.

Growth, Purification, and Preparation of Y352F CYP158A2 (CYP158A2*) Compound I

CYP158A2* was obtained as reported previously.[6] CYP158A2*-I samples were prepared by reacting ferric protein (6 mM, Rz   2.00, in 100 mM tris-HCl buffer, pH 7.0) with a solution of *m*-CPBA (24 mM, 30% acetonitrile) in a 2:1 mixture (v/v). Reactants were mixed and quenched into liquid ethane ~ 2 ms after mixing. Samples were packed into Mössbauer and EXAFS sample cups for spectroscopic analysis at a final protein concentration of 4 mM. The final concentrations of *m*-CPBA and acetonitrile were 8 mM and 10% (v/v), respectively.

Purification of Chloroperoxidase

Chloroperoxidase was obtained from the filamentous fungus *Caldariomyces fumago* (ATCC 16373) and purified according to established protocols.[19] Protein fractions with an R_Z (Abs_{400nm}/Abs_{280nm}) value of   1.45 were used for experiments.

CPO-I Preparation

CPO-I samples for VTM and XAS measurements were prepared as previously described[19] with slight modifications by reacting ~7 mM ferric CPO with ~150 mM peracetic acid, both in 100 mM potassium phosphate (Kphos) buffer pH 6.5, in a 2:1 mixture. The pH of the peracetic acid solution was adjusted back to pH 6.5 after the addition of peracetic acid. The aqueous reaction mixture was sprayed into liquid ethane (90 K) ~2 ms after mixing. Liquid ethane was removed under vacuum in an isopentane bath (~128 K), after which samples were packed into Mössbauer or EXAFS cups under liquid nitrogen.

Stopped-Flow Kinetics Measurements

Kinetic experiments with CYP119A1, experimental setup, and data analyses were similar to those described previously.[5] In a typical kinetic experiment involving CPO, an aqueous solution containing 100 mM Kphos (pH 4.0) and 20 μM CPO was mixed with an aqueous solution of 20 μM peracetic acid and aged until exponential decay of compound I was

apparent (2 seconds). The resulting solution, typically consisting of ~60% CPO-I, was then mixed with a buffered (pH 4.0) aqueous solution of 5-hexenoic acid or hexanoic acid (0-24 mM). The decay of CPO-I was monitored at 690 nm.

Mössbauer Data Collection and Analysis

Mössbauer spectra were recorded on a spectrometer from SEE CO (formerly WEB research) operating in constant acceleration mode in transmission geometry. The sample was kept inside an SVT-400 dewar from Janis with a magnetic field of 54 mT applied parallel to the γ-beam. Spectra were recorded at the indicated temperatures. The quoted isomer shifts are relative to the centroid of the spectrum of a metallic foil of α-Fe at room temperature. Temperature studies for each sample (CPO-I, CYP119A1-I, and ferric CYP119A1) were performed in duplicate. Data analysis was performed using the program WMOSS from WEB research. Analysis of variable temperature data was performed with a modified version of the FORTRAN program CPLRXF by C. Schulz, using methodology described by Schulz et al.[42] No assumptions about the nature of the relaxation process were made. Instead, the relaxation rate (W) was provided externally and then used directly to construct the relaxation matrix. CPLRXF was interfaced and fitting was performed through the MATLAB programming environment.

XAS Sample Preparation

All XAS samples were prepared in modified Mössbauer cups. The bottom of each cup was removed, and the opening was covered with Kapton tape. Freeze-quenched protein was packed into the modified cups under liquid nitrogen. Samples were stored in liquid nitrogen until XAS measurements were performed.

XAS Data Collection and Analysis

X-ray absorption measurements were performed at the Stanford Synchrotron Radiation Laboratory (SSRL) on beam line 7-3 at ~ 10 K as previously described with slight modifications.[6] The data were collected by using a Si(220) $\phi = 0°$ double-crystal monochromator with a 9.0 keV cutoff for harmonic rejection. Data sets were collected in fluorescence mode with a 30-element Ge detector.

To avoid photoreduction during XAS measurements, the sample position in the beam was adjusted after each scan so that a previously unexposed portion of the sample was examined. Each EXAFS data set consisted of ~20 first scans. All CYP119A1-I and CYP119A2-I samples contained ~70% compound I as judged by Mössbauer spectroscopy (the remainder was ferric enzyme). CYP158A2*-I contained ~85% compound I, while CPO-I samples contained   95% compound I.

Raw XAS data were fit over the region k=3–15. Fits, performed as previously described with some modifications,[3,19] included first and second shell atoms and one multiple-scattering component. In all cases, the second shell was comprised of α- and meso- carbons and the Fe–C_α–N–Fe multiple-scattering paths (N = 8, 4, and 16, respectively). The scale factor, S_0, was set to 0.9. Fits of the CYP119A1-I and CYP119A2-I data accounted for a ~30% ferric component by including a Fe-S scattering path fixed at the Fe-S distance

obtained from experiments on ferric P450. The ability to resolve two similar (i.e. both Fe-S) but different scattering paths in EXAFS experiments is determined by the resolution of the experiment. The resolution in EXAFS is given by the formula $r \approx \pi/(2*k)$, where r is the difference in the two path lengths and k is k-range over which data is fit. Our EXAFS data were fit from k=3-15 Å^{-1}, giving a resolution of 0.13 Å. This means the two scattering paths must differ by 0.13 Å for us to be able to resolve and identify their individual contributions. The difference between the Fe-S distances found in ferric enzyme and compound I is 0.18 Å, (0.05 Å longer than required). Thus, the ferric component of the sample does not affect our measurement of the compound I Fe-S distance. The two scattering contributions can be readily resolved. The results obtained from fitting each independent sample were averaged to obtain final metal-ligand distances and standard deviations. Energies were calibrated using an iron foil (7111.2 eV) and edge positions were obtained from the first derivative of the data using EXAFSPAK (1.0 eV smoothing, third-order polynomial).

Pre-edge data was fit using the EDG_FIT portion of EXAFSPAK.[50] Pre-edge peaks were modeled with pseudo-Voigt shaped lines set to a 50:50 (Lorentzian: Gaussian) ratio. Fits of multiple energy ranges were averaged to obtain pre-edge areas. In addition, some of the fits included a post edge or background curve that was allowed to vary.[43] Areas of the fits were determined using the method of Westre *et al.*[41] Fits of the P450-I data contained a ferric component with parameters constrained to the values obtained from fits of the ferric data. Pre-edge calculations were performed using methods outlined by DeBeer and Neese with minor modifications (SI).[43]

Supplementary Material

Refer to Web version on PubMed Central for supplementary material.

Acknowledgements

References

1. Groves JT. Enzymatic C-H Bond Activation Using Push to Get Pull. Nature Chem. 2014; 6:89–91. [PubMed: 24451580]

2. Dawson JH. Probing Structure-Function Relations in Heme-Containing Oxygenases and Peroxidases. Science. 1988; 240:433–439. [PubMed: 3358128]

3. Green MT, Dawson JH, Gray HB. Oxoiron(IV) in chloroperoxidase compound II is basic: Implications for P450 chemistry. Science. 2004; 304:1653–1656. [PubMed: 15192224]

4. Green MT. C-H bond activation in heme proteins: the role of thiolate ligation in cytochrome P450. Curr. Opin. Chem. Biol. 2009; 13:84–88. [PubMed: 19345605]

5. Rittle J, Green MT. Cytochrome P450 Compound I: Capture, Characterization, and C-H Bond Activation Kinetics. Science. 2010; 330:933–937. [PubMed: 21071661]

6. Yosca TH, et al. Iron(IV)hydroxide pK(a) and the Role of Thiolate Ligation in C-H Bond Activation by Cytochrome P450. Science. 2013; 342:825–829. [PubMed: 24233717]

7. Krest CM, et al. Reactive Intermediates in Cytochrome P450 Catalysis. J. Biol. Chem. 2013; 288:17074–17081. [PubMed: 23632017]

8. McQuarters AB, Wolf MW, Hunt AP, Lehnert N. 1958-2014: After 56 Years of Research, Cytochrome P450 Reactivity Is Finally Explained. Angew. Chem., Int. Ed. 2014; 53:4750–4752.

9. Jung C. The mystery of cytochrome P450 Compound I A mini-review dedicated to Klaus Ruckpaul. Biochim. Biophys. Acta, Proteins Proteomics. 2011; 1814:46–57.

10. Gross Z, Nimri S. A Pronounced Axial Ligand Effect on the Reactivity of Oxoiron(IV) Porphyrin Cation Radicals. Inorg. Chem. 1994; 33:1731–1732.

11. Song WJ, Ryu YO, Song R, Nam W. Oxoiron(IV) porphyrin π-cation radical complexes with a chameleon behavior in cytochrome P450 model reactions. J. Biol. Inorg. Chem. 2005; 10:294–304. [PubMed: 15827730]

12. Kamachi T, Kouno T, Nam W, Yoshizawa K. How axial ligands control the reactivity of high-valent iron(IV)-oxo porphyrin π-cation radicals in alkane hydroxylation: A computational study. J. Inorg. Biochem. 2006; 100:751–754. [PubMed: 16516298]

13. Kang Y, et al. Enhanced Reactivities of Iron(IV)-Oxo Porphyrin π-Cation Radicals in Oxygenation Reactions by Electron-Donating Axial Ligands. Chem.--Eur. J. 2009; 15:10039–10046. [PubMed: 19697378]

14. Prokop KA, de Visser SP, Goldberg DP. Unprecedented Rate Enhancements of Hydrogen-Atom Transfer to a Manganese(V)-Oxo Corrolazine Complex. Angew. Chem., Int. Ed. 2010; 49:5091–5095.

15. Urano Y, Higuchi T, Hirobe M, Nagano T. A pronounced axial thiolate ligand effect on the reactivity of the high valent oxo-iron porphyrin intermediate. FASEB J. 1997; 11:A817–A817.

16. Ohno T, et al. Remarkable axial thiolate ligand effect on the oxidation of hydrocarbons by active intermediate of iron porphyrin and cytochrome P450. J. Inorg. Biochem. 2000; 82:123–125. [PubMed: 11132618]

17. van Rantwijk F, Sheldon RA. Selective oxygen transfer catalysed by heme peroxidases: synthetic and mechanistic aspects. Curr. Opin. Biotechnol. 2000; 11:554–564. [PubMed: 11102789]

18. Rutter R, et al. Chloroperoxidase Compound-I - Electron-Paramagnetic Resonance and Mössbauer Studies. Biochemistry. 1984; 23:6809–6816. [PubMed: 6099143]

19. Stone KL, Behan RK, Green MT. X-ray absorption spectroscopy of chloroperoxidase compound I: Insight into the reactive intermediate of P450 chemistry. Proc. Natl. Acad. Sci. U. S. A. 2005; 102:16563–16565. [PubMed: 16275918]

20. Sundaramoorthy M, Terner J, Poulos TL. The crystal structure of chloroperoxidase: A heme peroxidase-cytochrome P450 functional hybrid. Structure. 1995; 3:1367–1377. [PubMed: 8747463]

21. Poulos TL, Finzel BC, Howard AJ. High-Resolution Crystal-Structure of Cytochrome-P450cam. J. Mol. Biol. 1987; 195:687–700. [PubMed: 3656428]

22. Zaks A, Dodds DR. Chloroperoxidase-Catalyzed Asymmetric Oxidations - Substrate-Specificity and Mechanistic Study. J. Am. Chem. Soc. 1995; 117:10419–10424.

23. Zhang R, Nagraj N, Lansakara DSP, Hager LP, Newcomb M. Kinetics of two-electron oxidations by the Compound I derivative of chloroperoxidase, a model for cytochrome P450 oxidants. Org. Lett. 2006; 8:2731–2734. [PubMed: 16774243]

24. Ueyama N, Nishikawa N, Yamada Y, Okamura T, Nakamura A. Cytochrome P-450 model (porphinato)(thiolato)iron(III) complexes with single and double NH•••S hydrogen bonds at the thiolate site. J. Am. Chem. Soc. 1996; 118:12826–12827.

25. Ueyama N, et al. Synthesis and properties of octaethylporphinato(arenethiolato)iron(III) complexes with intramolecular NH - S hydrogen bond: Chemical function of the hydrogen bond. Inorg. Chem. 1998; 37:2415–2421.

26. Suzuki N, et al. Novel iron porphyrin-alkanethiolate complex with intramolecular NH•••S hydrogen bond: Synthesis, spectroscopy, and reactivity. J. Am. Chem. Soc. 1999; 121:11571–11572.

27. Ueno T, et al. Role of the invariant peptide fragment forming NH•••S hydrogen bonds in the active site of cytochrome P-450 and chloroperoxidase: Synthesis and properties of Cys-containing peptide Fe(III) and Ga(III) (octaethylporphinato) complexes as models. Inorg. Chem. 1999; 38:1199–1210. [PubMed: 11670903]

28. Yoshioka S, et al. Roles of the proximal hydrogen bonding network in cytochrome P450(cam)-catalyzed oxygenation. J. Am. Chem. Soc. 2002; 124:14571–14579. [PubMed: 12465966]

29. Dey A, et al. Sulfur K-edge XAS and DFT calculations on P450 model complexes: Effects of hydrogen bonding on electronic structure and redox potentials. J. Am. Chem. Soc. 2005; 127:12046–12053. [PubMed: 16117545]

30. Matsumura H, et al. Modulation of redox potential and alteration in reactivity via the peroxide shunt pathway by mutation of cytochrome P450 around the proximal heme ligand. Biochemistry. 2008; 47:4834–4842. [PubMed: 18363338]

31. Dey A, et al. S K-edge XAS and DFT Calculations on Cytochrome P450: Covalent and Ionic Contributions to the Cysteine-Fe Bond and Their Contribution to Reactivity. J. Am. Chem. Soc. 2009; 131:7869–7878. [PubMed: 19438234]

32. Galinato MGI, Spolitak T, Ballou DP, Lehnert N. Elucidating the Role of the Proximal Cysteine Hydrogen-Bonding Network in Ferric Cytochrome P450cam and Corresponding Mutants Using Magnetic Circular Dichroism Spectroscopy. Biochemistry. 2011; 50:1053–1069. [PubMed: 21158478]

33. Lehnert N. Elucidating second coordination sphere effects in heme proteins using low-temperature magnetic circular dichroism spectroscopy. J. Inorg. Biochem. 2012; 110:83–93. [PubMed: 22516139]

34. Park SY, et al. Thermophilic cytochrome P450 (CYP119) from Sulfolobus solfataricus: high resolution structure and functional properties. J. Inorg. Biochem. 2002; 91:491–501. [PubMed: 12237217]

35. Beitlich T, Kuhnel K, Schulze-Briese C, Shoeman RL, Schlichting I. Cryoradiolytic reduction of crystalline heme proteins: analysis by UV-Vis spectroscopy and X-ray crystallography. J. Synchrotron Radiat. 2007; 14:11–23. [PubMed: 17211068]

36. While CYP119A1-I reactions have been exclusively conducted at pH 7.0, chloroperoxidase is unstable under these alkaline conditions. CPO-I is stable at lower pH ranges and the reaction of 5-hexenoic acid with CPO-I was examined at pH's of 4.0 – 6.5. The highest reaction rates are observed at pH 4.0 and these are the values quoted.

37. Green MT. Imidazole-ligated compound I intermediates: The effects of hydrogen bonding. J. Am. Chem. Soc. 2000; 122:9495–9499.

38. Green MT. The structure and spin coupling of catalase compound I: A study of noncovalent effects. J. Am. Chem. Soc. 2001; 123:9218–9219. [PubMed: 11552853]

39. Weiss R, et al. Delocalization over the heme and the axial ligands of one of the two oxidizing equivalents stored above the ferric state in the peroxidase and catalase Compound-I intermediates: Indirect participation of the proximal axial ligand of iron in the oxidation reactions catalyzed by hemebased peroxidases and catalases? J. Biol. Inorg. Chem. 1996; 1:377–383.

40. Green MT. Evidence for sulfur-based radicals in thiolate compound I intermediates. J. Am. Chem. Soc. 1999; 121:7939–7940.

41. Schulz CE, Nyman P, Debrunner PG. Spin Fluctuations of Paramagnetic Iron Centers in Proteins and Model Complexes - Mössbauer and EPR Results. J. Chem. Phys. 1987; 87:5077–5091.

42. Winkler H, Schulz C, Debrunner PG. Spin Fluctuation Rates from Mössbauer-Spectra of High-Spin Ferrous Rubredoxin. Phys. Lett. A. 1979; 69:360–363.

43. Chandrasekaran P, et al. Prediction of high-valent iron K-edge absorption spectra by time-dependent Density Functional Theory. Dalton Trans. 2011; 40:11070–11079. [PubMed: 21956429]

44. Westre TE, et al. A multiplet analysis of Fe K-edge 1s→ 3d pre-edge features of iron complexes. J. Am. Chem. Soc. 1997; 119:6297–6314.

45. Spiro TG, Wasbotten IH. CO as a vibrational probe of heme protein active sites. J. Inorg. Biochem. 2005; 99:34–44. [PubMed: 15598489]

46. Mak PJ, Yang YT, Im S, Waskell LA, Kincaid JR. Experimental Documentation of the Structural Consequences of Hydrogen-Bonding Interactions to the Proximal Cysteine of a Cytochrome P450. Angew. Chem., Int. Ed. 2012; 51:10403–10407.

47. Hollenberg PF, Hager LP, Blumberg WE, Peisach J. An Electron-Paramagnetic Resonance Study of the High and Low-Spin Forms of Chloroperoxidase. J. Biol. Chem. 1980; 255:4801–4807. [PubMed: 6246083]

48. Paulat F, Lehnert N. Electronic structure of ferric heme nitrosyl complexes with thiolate coordination. Inorg. Chem. 2007; 46:1547–1549. [PubMed: 17286401]

49. Williams-Smith DL, Bray RC, Barber MJ, Tsopanakis AD, Vincent SP. Changes in Apparent Ph on Freezing Aqueous Buffer Solutions and Their Relevance to Biochemical Electron-Paramagnetic-Resonance Spectroscopy. Biochem. J. 1977; 167:593–600. [PubMed: 23760]
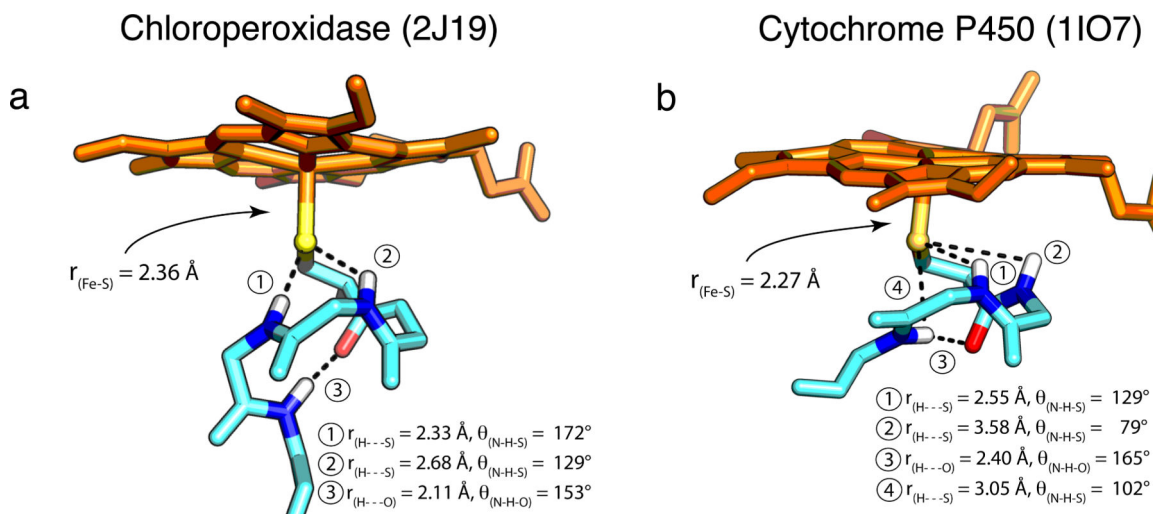
50. George, GN. EXAFSPAK. 2000. http://ssrl.slac.stanford.edu/exafspak.html

Chloroperoxidase (2J19)

$r_{(Fe-S)} = 2.36$ Å

① $r_{(H\cdots S)} = 2.33$ Å, $\theta_{(N-H-S)} = 172°$
② $r_{(H\cdots S)} = 2.68$ Å, $\theta_{(N-H-S)} = 129°$
③ $r_{(H\cdots O)} = 2.11$ Å, $\theta_{(N-H-O)} = 153°$

Cytochrome P450 (1IO7)

$r_{(Fe-S)} = 2.27$ Å

① $r_{(H\cdots S)} = 2.55$ Å, $\theta_{(N-H-S)} = 129°$
② $r_{(H\cdots S)} = 3.58$ Å, $\theta_{(N-H-S)} = 79°$
③ $r_{(H\cdots O)} = 2.40$ Å, $\theta_{(N-H-O)} = 165°$
④ $r_{(H\cdots S)} = 3.05$ Å, $\theta_{(N-H-S)} = 102°$

Figure 1.
P450 displays weaker/poorer H-bonding interactions compared to CPO. H-bonding metrics and Fe-S distances from the crystal structures of (a) ferric CPO (2J19) and (b) ferric CYP119A1 (1IO7) are shown. The H-bonding metrics for CYP119A1 are typical of P450s. Average distances (angles) for the four P450s discussed in this paper [CYP119A1, CYP119A2 (3B4X), CYP158A2 (1SE6), and CYP101 (1PHC)] are: ① 2.59±0.12Å (124±3°); ② 3.59±0.08Å (76±4°); ③ 2.41±0.25Å (161±6°); ④ 3.09±0.18Å (99±3°). Protein Data Bank accession codes for each structure are given in parentheses.
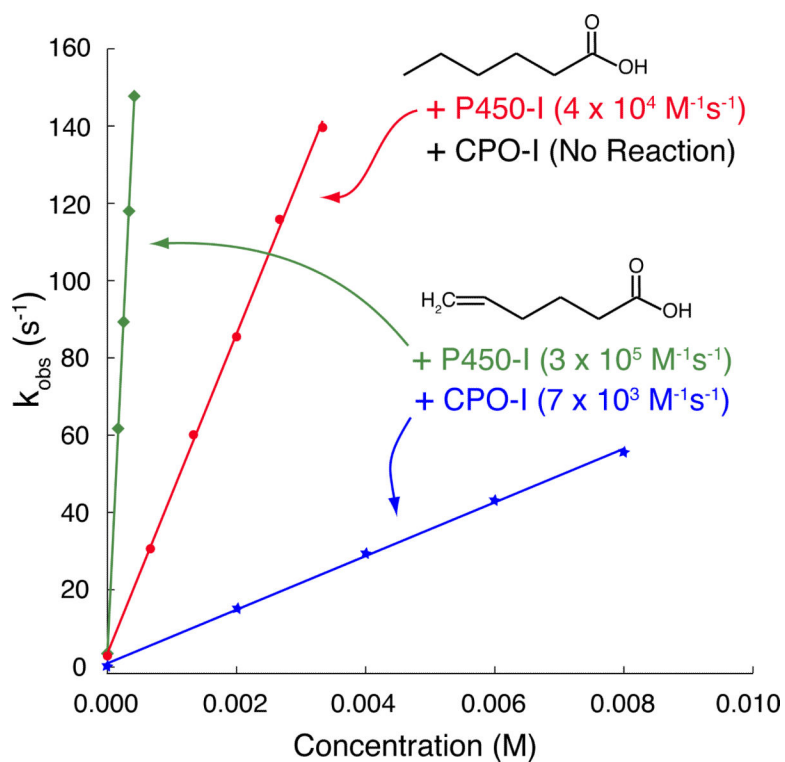
Figure 2.
Rates of substrate oxidation by CPO-I and CYP119A1-I. Both CPO-I and P450-I readily epoxidize 5-hexenoic acid, indicating that the aliphatic termini of fatty acids can reach the ferryl moiety. Yet, only P450-I reacts with hexanoic acid, hydroxylating it at the ω-1 position. This disparity in C-H bond hydroxylating competence suggests an inherent difference in the reactivity of compound I in P450 and CPO. Experimental details are given in Methods.
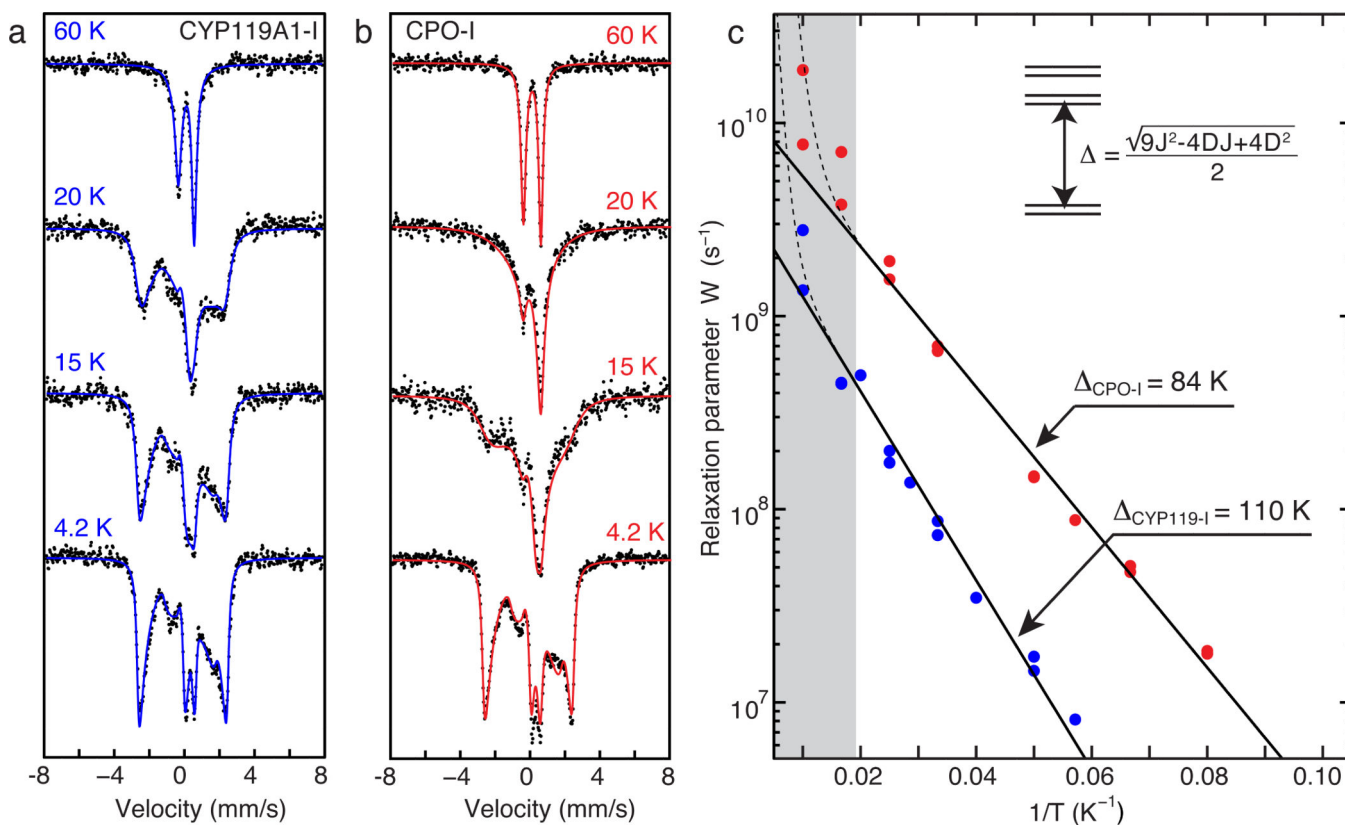
Figure 3.
Variable temperature Mössbauer data for (a) CYP119A1-I and (b) CPO-I. With increasing temperature, the Mössbauer spectrum of CPO-I collapses towards a quadrupole doublet more quickly than that of P450-I, indicating that P450-I has a slower electronic relaxation rate than CPO-I. Fits of the data shown in (c) reveal that a larger exchange coupling is responsible for the slower relaxation. The contributions from ferric enzyme were subtracted from each spectrum in (a). The splitting between the lowest Kramers doublets ( ) was obtained by fitting the linear region in (c) to Eq. 1. The grey bar indicates the temperature range in which Raman relaxation modes begin to dominate the Orbach mechanism. A complete listing of Mössbauer paramaters and relaxation rates can be found in Supplementary Tables S1 and S2.
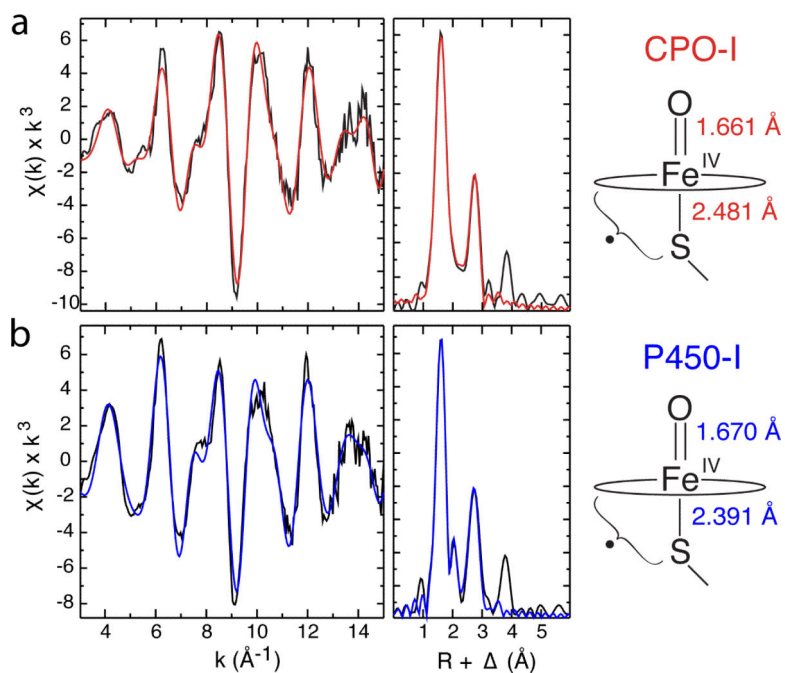
Figure 4.
Representative Fe K-edge EXAFS data and Fourier transforms for CPO-I (a) and
CYP119A1-I (b). Raw data are shown in black and best fits are shown in red and blue,
respectively. The distances shown at the right were obtained by averaging independent
measurements for CPO-I and P450-I (CYP119A1-I, CYP119A2-I, and CYP158A2*-I).
These distances reveal that the Fe-S bond in P450-I is significantly shorter than in CPO-I,
suggesting more electron donation from the proximal thiolate ligand to the ferryl moiety in
P450. This may in part explain P450's greater propensity for C-H bond activation.

Table 1

Best fits for compound I EXAFS data. Each row corresponds to a best fit for data obtained from measurements on an independently prepared set of samples.

	Fe-N			Fe-S			Fe-O				
	N	R	σ^2	N	R	σ^2	N	R	σ^2	E_0	Error
CPO-I	4	2.004	0.0011	1	2.469	0.0031	1	1.661	0.0011	−12.4	0.286
	4	2.006	0.0010	1	2.472	0.0040	1	1.658	0.0029	−12.1	0.346
	4	2.001	0.0018	1	2.511	0.0129	1	1.667	0.0018	−12.3	0.331
	4	2.000	0.0021	1	2.472	0.0069	1	1.658	0.0047	−13.2	0.331
Average		**2.003**			**2.481**			**1.661**			
90% Conf. Interval		**0.003**			**0.023**			**0.005**			
CYP119A1-I	4	2.003	0.0015	0.75	2.397	0.0045	0.75	1.667	0.0027	−12.5	0.264
	4	1.998	0.0016	0.75	2.392	0.0045	0.75	1.672	0.0020	−13.7	0.352
	4	1.993	0.0013	0.65	2.374	0.0037	0.65	1.673	0.0032	−15.3	0.316
Average		**1.998**			**2.388**			**1.670**			
90% Conf. Interval		**0.008**			**0.020**			**0.006**			
CYP119A2-I	4	1.996	0.0017	0.65	2.386	0.0067	0.65	1.669	0.0027	−14.2	0.305
CPY158A2*-I	4	2.010	0.0016	1	2.405	0.0102	1	1.669	0.0042	−13.4	0.364
Avg. (all P450S)		**2.000**			**2.391**			**1.670**			
90% Conf. Interval		**0.006**			**0.011**			**0.002**			

X-ray absorption fine structure measurements on the compound I forms of cytochrome P450 (P450) and chloroperoxidase (CPO) reveal that the Fe-S bond is significantly shorter (~0.1 Å) in P450 than in CPO. Increased electron donation from the axial thiolate ligand may explain P450's greater propensity for C-H bond activation.